Geosci. Model Dev. Discuss., 8, 8155–8191, 2015
www.geosci-model-dev-discuss.net/8/8155/2015/
doi:10.5194/gmdd-8-8155-2015

Geoscientific Model Development Discussions
Open Access

ESCIMO.spread (v2): parameterization of a spreadsheet-based energy balance snow model for inside-canopy conditions

T. Marke[1], E. Mair[1], K. Förster[3], F. Hanzer[1,3], J. Garvelmann[2], S. Pohl[4], M. Warscher[2], and U. Strasser[1]

[1]Institute of Geography, University of Innsbruck, Innsbruck, Austria
[2]Institute of Meteorology and Climate Research (IMK-IFU), Karlsruhe Institute of Technology (KIT), Garmisch-Partenkirchen, Germany
[3]alpS – Centre for Climate Change Adaptation, Innsbruck, Austria
[4]Hydrology Department, University of Freiburg, Freiburg, Germany

Received: 30 June 2015 – Accepted: 13 August 2015 – Published: 25 September 2015

Correspondence to: T. Marke (thomas.marke@uibk.ac.at)

Published by Copernicus Publications on behalf of the European Geosciences Union.

Abstract

This article describes the extension of the spreadsheet-based point energy balance snow model ESCIMO.spread by (i) an advanced approach for precipitation phase detection, (ii) a concept for cold and liquid water storage consideration and (iii) a canopy sub-model that allows to quantify the effect of a forest canopy on the meteorological conditions inside the forest as well as the simulation of snow accumulation and ablation inside a forest stand. To provide the data for model application and evaluation, innovative low-cost Snow Monitoring Systems (SnoMoS) have been utilized that allow the collection of important meteorological and snow information in and outside the canopy. The model performance with respect to both, the modification of meteorological conditions as well as the subsequent calculation of the snow cover evolution are evaluated using in- and outside-canopy observations of meteorological variables and snow cover evolution as provided by a pair of SnoMoS for a site in the Black Forest mountain range (south-west Germany). The validation results indicate a good overall model performance in and outside the forest canopy. The newly developed version of the model refered to as ESCIMO.spread (v2) is provided free of charge together with one year of sample data including the meteorological data and snow observations used in this study.

1 Introduction

In forested areas significant variations in snow accumulation can result from the processes of forest canopy interception and sublimation of intercepted snow (Marsh, 1999; Pomeroy et al., 1998). Snowfall in forested areas is either intercepted by stems, needles and branches or passes through the canopy directly reaching the underlying forest floor. Due to its large surface area exposed to the surrounding atmosphere, intercepted snow can be subject to high sublimation losses, especially in dry continental climates. Generally, sublimation losses of previously intercepted snow can be as high as 30 %

GMDD
8, 8155–8191, 2015

of snow precipitation, depending on the efficiency of interception, its duration and the atmospheric boundary conditions (Liston and Elder, 2006b; Pomeroy and Gray, 1995; Strasser et al., 2008). Intercepted snow can also be removed from the canopy by direct unloading and dripping of meltwater to the ground (Liston and Elder, 2006b; Pomeroy et al., 2002). Compared to snow in the open, snow in forest canopies is exposed to different meteorological conditions. It is sheltered from wind and incoming shortwave radiation while receiving increased longwave radiation emitted from the surrounding trees (Link and Marks, 1999a, b). Likewise, humidity and temperature underneath a canopy differ from those in the open (Liston and Elder, 2006b). In the boundary layer, forest canopies moreover strongly modify the interactions between snow-covered surfaces and the atmosphere. Even the litter on the forest floor has a significant effect on the radiative properties of the snow cover beneath a canopy (Melloh et al., 2002; Hardy et al., 2001).

The influences of a forest canopy on the snow cover dynamics beneath are very complex. The snow cover duration in the forest depends on various factors. A delay of the spring snow melt under a dense forest canopy compared to open areas due to the reduction of incoming solar radiation was shown by Link and Marks (1999a). On the other hand shorter snowpack duration in the forest was observed by Dickerson-Lange et al. (2015). Strasser et al. (2011) showed in a numerical modelling experiment for a virtual mountain that in snow-rich winters, the shadowing and its protective effect is dominant. In winters with little snow, snow sublimation losses become dominant and, consequently, the snow lasts longer in the open than inside the forest, mainly for northern exposures (in the Northern Hemisphere). Similar patterns were observed by Pohl et al. (2014) in the Black Forest region.

To develop a free and easy to use tool for the simulation of the temporal evolution of the snow cover with explicit consideration of these complex snow-canopy-atmosphere interactions, the spreadsheet-based point energy balance snow model ESCIMO.spread (Strasser and Marke, 2010) has been extended with a canopy sub-model. Moreover, the model has been improved by integrating an advanced algorithm for precipitation phase detection that applies wet-bulb temperature as a criterion to distinguish solid and liquid precipitation. Another model improvement is a new parameterization for cold and liquid water content of the snow cover allowing to consider refreezing of rain or meltwater in the snowpack. Compared to other existing spreadsheet-based snow models (e.g. the glacier and snow melt study model by Brock and Arnold, 2000) ESCIMO.spread (v2) is particularly fast and can easily be modified by simple change of the parameters and formulae with results immediately visualized. The model requires only few input data (hourly recordings of temperature, precipitation, wind speed, relative humidity, global as well as longwave radiation) and is even capable of simulating the evolution of a seasonal snow cover under climate change conditions. The latter is realized by defining trends in precipitation and/or temperature in the models parameter section. While Walter et al. (2005) have presented a spreadsheet energy balance model that requires even less meteorological input data (daily minimum/maximum temperature and precipitation), their approach operates at a daily time step only and does not allow to quantify sub-daily variations in snow cover conditions. Moreover, compared to the canopy model implemented in ESCIMO.spread (v2), the consideration of canopy effects in the Walter et al. (2005) model is reduced to a canopy-induced extinction of solar radiation only. Canopy effects on other meteorological variables or vegetation-snow cover interactions (e.g. the interception of snow in the canopy) are not accounted for. As ESCIMO.spread (v2) is in simple table format and does not include any macros it can be applied by all common spreadsheet programs (e.g., Microsoft Excel, Apple Numbers, OpenOffice Calc) on a variety of platforms (Windows, Linux, Mac OS). Due to its simplicity, ESCIMO.spread (v2) is particularly suitable for application in education (e.g., in practically-oriented student courses) and can even be operated with laptop computers, e.g. to visualize and plausify measured meteorological parameters and the simulated snow cover directly in the field.

With its new features of

– sophisticated precipitation phase detection using a wet bulb temperature threshold,

– cold content and liquid water content calculation with consideration of refreezing of water from melt or rain, and meltwater outflow,

– transformation of standard meteorological observations (precipitation, relative humidity, temperature, wind speed, global radiation) from the open into conditions inside a forest canopy,

– calculation of snow interception and subsequent sublimation, melt or dropping of intercepted snow to the ground and

– calculation of the beneath-canopy snow energy and mass balance,

the new version ESCIMO.spread (v2) reaches beyond the capabilities of most other freely available point-scale snow models and can be expected to set forth the history of ESCIMO.spread as a well-accepted, documented and freely available snow model for application in both science and education. This paper describes the newly implemented algorithms and evaluates the model results against available hydrometeorological observations in and outside the forest canopy at a site in the Black Forest mountain range (south-west Germany, see Fig. 1) with a mostly temperate snow cover in an elevation of 800 m a.s.l. The applied hydrometeorological data have been recorded by a set of low-cost snow monitoring systems (SnoMoS) recently developed by Pohl et al. (2014). The model can be downloaded from www.alpinehydroclimatology.net together with one year of example meteorological recordings and snow observations.

2 The ESCIMO.spread model (v2)

2.1 General description

The new version ESCIMO.spread (v2) builds upon the ESCIMO.spread model as published by Strasser and Marke (2010). It is a 1-D, one-layer process model which calculates snow accumulation and melt for a snow cover assumed to be a single and homogeneous pack. To do so, it solves the energy and mass balance equations for the snow surface applying simple parameterizations of the relevant processes. The energy balance of the snow surface is calculated for each hourly time step considering short- and longwave radiation, sensible and latent heat fluxes, energy conducted by solid or liquid precipitation as well as sublimation/resublimation and a constant soil heat flux (Strasser and Marke, 2010). Thereby, absorbed and reflected shortwave radiation is calculated from incoming shortwave radiation on the basis of the snow albedo, which is estimated for each hourly time step using an albedo ageing curve approach. Solid precipitation increases the amount of snow water equivalent (SWE) on the land surface, while liquid precipitation is (up to a certain maximum amount depending on actual SWE) added to the liquid water storage of the snowpack. Melt is calculated from the energy balance remainder if air temperature exceeds 273.16 K, whereas no melt is assumed to occur for air temperatures below 273.16 K. The model results are visualized in the form of diagrams for the majority of model variables, together with three quantitative measures of goodness of fit.

2.2 Precipitation phase detection

The new version of ESCIMO.spread (v2) includes an improved distinction between liquid and solid precipitation. As air temperature T_a is often an insufficient indicator for the precipitation water phase (Steinacker, 1983), wet-bulb temperature T_w is used in ESCIMO.spread (v2) as a combined measure of air temperature and humidity to distinguish rain from snowfall. Figure 2 shows the relation between air temperature, wet-bulb temperature and relative humidity for different altitudes to account for the dependence of wet-bulb pressure on air pressure. Each of the displayed lines in Fig. 2 could be interpreted as a borderline to separate liquid and solid precipitation assuming a certain threshold wet-bulb temperature. Largest differences between air temperature and wet-bulb temperature occur at low air humidities, clearly pronouncing the added value associated to application of wet-bulb temperature as a criterion for phase detection.

Generally, wet-bulb temperature can be derived by solving the psychrometric equation

$$e_a(T_a) - e_s(T_w) - A \times (T_a - T_w) = 0 \quad (1)$$

for T_w (K), where A (Pa K^{-1}) is the psychrometric constant, and $e_a(T_w)$ (Pa) and $e_s(T_w)$ (Pa) the vapor pressure of the air and the saturation vapor pressure at wet-bulb temperature, respectively. As there is no explicit solution to the psychrometric equation (Campbell and Norman, 1998) and iterations are unfavourable in a spreadsheet model, a pragmatic assumption has been made: for a broad range of combinations of air temperature and relative humidity values, lookup tables have been generated outside the spreadsheet model using an iterative solution scheme for Eq. (1). Beside temperature and humidity, wet-bulb temperature also depends on air pressure p_z (Pa) which is required to calculate the psychrometric constant, A, as (Kraus, 2004)

$$A = \frac{p_z \times c_p}{0.622 \times L_v}, \quad (2)$$

where c_p is the specific heat capacity of air at constant pressure (1004 J kg^{-1} K^{-1}) and L_v (J kg^{-1}) represents the latent heat of vaporization. In ESCIMO.spread (v2) the temperature dependence of the psychrometric constant is neglected since this dependency is by far less important compared to that associated to air pressure at higher altitudes (Kraus, 2004; Campbell and Norman, 1998). Air pressure, p (hPa), at a given elevation, z (m), can be derived from standard atmospheric pressure, p_0 (= 1013 hPa), by integration of the hydrostatic equation assuming a linear decrease of temperature with increasing altitude ($\gamma = -0.0065$ K m^{-1})

$$p_z = p_0 \left[\frac{T_a}{T_a - \gamma \times z}\right]^{-\frac{g}{\gamma \times R}}, \quad (3)$$

where R is the gas constant of dry air (287 J kg^{-1} K^{-1}) and g is gravity (m s^{-2}). To account for the air pressure dependence, the implemented lookup tables have been prepared for several elevation bands with a 500 m interval. Figure 3 shows a comparison of wet-bulb temperatures calculated using the lookup table approach to those achieved with an iterative solution for different elevations. The differences between both approaches shown for a common snowfall situation are relatively small. Therefore, the lookup table approach allows a sufficiently accurate estimation of wet-bulb temperature in the model. The threshold for wet-bulb temperature as required for precipitation phase detection in ESCIMO.spread (v2) is one of the user-defined input parameters and is here set to 273.16 K.

2.3 Cold and liquid water content

A conceptual parameterization for the liquid water and cold content of the snowpack based on Braun (1984) and Blöschl and Kirnbauer (1991) has been added to the model. Heat losses resulting from a negative energy balance are thereby used to build up a cold content, which first needs to be reduced to zero by positive energy inputs before actual melt can occur. Conversely, melting snow is not immediately removed from the snowpack, but a certain amount of liquid water can be retained (and possibly refreeze again). This approach accounts for the delay between beginning surface melt and drainage of a snow cover.

Three model parameters control these processes: the water holding capacity, HC_w (–), the cold holding capacity, HC_c (–) (both specified as a fraction of the total snowpack weight), and the refreezing factor, F_r (–), which is the fraction of the computed heat loss used for refreezing and building up the cold content. By default, these parameters are set as recommended by Blöschl and Kirnbauer (1991) to $HC_w = 0.1$, $HC_c = 0.03$, and $F_r = 0.5$.

The potential melt, M_p (mm) is calculated using the available melt energy, M (J), as

$$M_p = \frac{M}{c_i}, \tag{4}$$

where c_i is the melting heat of ice (3337×10^5 J kg^{-1}).

GMDD
8, 8155–8191, 2015

In the case of a negative energy balance ($M < 0$), this "negative melt" is first used to calculate a refreezing of liquid water in the snowpack, RF (mm), in the form of

$$\mathrm{RF} = \min\left\{C_{\mathrm{lw}t-1}, -M_\mathrm{p} \times F_\mathrm{r}\right\}, \tag{5}$$

where $C_{\mathrm{lw}t-1}$ (mm) is the liquid water content of the previous time step. C_lw for a given time step is then derived as

$$C_\mathrm{lw} = C_{\mathrm{lw}t-1} + P_\mathrm{r} - \mathrm{RF}, \tag{6}$$

where P_r (mm) is liquid precipitation.

The remaining amount of energy is used to increase the cold content C_c (the cold content is represented with negative values, while the liquid water content is represented with positive values) as

$$C_\mathrm{c} = \max\left\{C_{\mathrm{c}t-1} + \left(M_\mathrm{p} \times F_\mathrm{r} + \mathrm{RF}\right), -\mathrm{HC_c} \times \mathrm{SWE}_{t-1}\right\}. \tag{7}$$

In the case of a positive energy balance ($M > 0$), first the sum of cold content reduction and actual melt is calculated as

$$M_\mathrm{v} = \min\left\{\mathrm{SWE}_{t-1} - C_{\mathrm{c}t-1}, M_\mathrm{p}\right\}. \tag{8}$$

C_c is then reduced with

$$C_\mathrm{c} = \min\left\{C_{\mathrm{c}t-1} + M_\mathrm{v}, 0\right\} \tag{9}$$

and actual melt, M_a (mm), is calculated as

$$M_\mathrm{a} = M_\mathrm{v} - \left(C_\mathrm{c} - C_{\mathrm{c}t-1}\right). \tag{10}$$

C_lw is then updated in the form of

$$C_\mathrm{lw} = \min\left\{C_{\mathrm{lw}t-1} + M_\mathrm{a}, \mathrm{SWE}_{t-1} \times \mathrm{HC_w}\right\} \tag{11}$$

and the outflow (i.e. the excess water that is actually removed from the snowpack), O (mm), is finally calculated as

$$O = \max\left\{\left(C_{\mathrm{lw}t-1} + P_\mathrm{r} + M_\mathrm{a}\right) - \mathrm{SWE}_{t-1} \times \mathrm{HC_w}, 0\right\}. \tag{12}$$

GMDD
8, 8155–8191, 2015

2.4 Modification of meteorological conditions inside the forest canopy

The canopy model newly implemented in ESCIMO.spread (v2) by Liston and Elder (2006b) has already been successfully applied under alpine conditions (see Strasser, 2008 or Strasser et al., 2011). The development of the approach was motivated by the fact that meteorological observations inside forest canopies only sparsely exist necessitating the estimation of inside-canopy conditions from availabe meteorological observations in the open. The method requires information on leaf area index and canopy height which can either be derived from field measurements or be taken from literature for a wide range of plant species (e.g. from Breuer et al., 2003, or Liston and Elder, 2006b).

Wind speed inside the canopy u_c ($\mathrm{m\,s^{-1}}$) is derived from above-canopy wind speed u ($\mathrm{m\,s^{-1}}$) as (Cionco, 1978)

$$u_c = u \exp(-a(1 - z/h)), \tag{13}$$

where h (m) is the canopy height and z (m) is the canopy reference level assumed to be 0.6 h (Liston and Elder, 2006b; Essery et al., 2003).

The canopy flow index, a (–) is calculated as a function of the effective leaf area index, LAI* ($\mathrm{m^2\,m^{-2}}$), and a scaling factor, β (= 0.9) that is introduced by Liston and Elder (2006b) to make LAI* compatible with the canopy flow index proposed by Cionco (1978):

$$a = \mathrm{LAI}^{*}\beta \tag{14}$$

LAI* includes stems, leaves and branches as described by Chen et al. (1997).

To consider the extinction of solar radiation by the forest canopy, top-of-canopy incoming shortwave radiation, Q_{si}, is reduced following the Beer–Lambert law as

$$Q_{sif} = Q_{si}\tau_v, \tag{15}$$

where Q_{sif} is the incoming shortwave radiation impinging on the snow surface beaneath the canopy (Hellström, 2001). τ_v representing the fraction of Q_{si} reaching the land surface is derived as

$$\tau_v = \exp(-k\mathrm{LAI}^*), \tag{16}$$

with k being a vegetation-dependent extinction coefficient (Liston and Elder, 2006b). Aiming at a best fit to observed radiation inside forest canopies of different species (e.g. spruce, subalpine fir, pine) at a site in the U.S. Department of Agriculture (USDA) Fraser Experimental Forest near Fraser (Colorado, USA), Liston and Elder (2006b) have yielded best overall performance using a k value of 0.71, which is also used for the simulations here.

Incoming longwave radiation inside the canopy is assumed to be composed by a fraction F_g (–) directly reaching the ground through gaps in the forest stand and a fraction F_c (–) emitted by the forest canopy. The canopy-emitted fraction is calculated following Liston and Elder (2006a) as

$$F_c = a + b\ln(\mathrm{LAI}^*) \tag{17}$$

where a (–) and b (–) are constants with values of 0.55 and 0.29, respectively. A value of F_g can be derived as

$$F_g = 1 - F_c, \tag{18}$$

with both calculated fractions used to estimate inside-canopy incoming longwave radiation Q_{lif} ($\mathrm{W\,m^{-2}}$) from

$$Q_{lif} = (F_g Q_{li}) + (F_c \sigma T_c^4), \tag{19}$$

where Q_{li} ($\mathrm{W\,m^{-2}}$) represents the top-of-canopy incoming longwave radiation. The latter is provided as input for ESCIMO.spread (v2) and is here estimated as a function of

GMDD
8, 8155–8191, 2015

A spreadsheet-based snow model for inside-canopy conditions

T. Marke et al.

temperature and cloud cover as proposed by Liston and Elder (2006a) due to a lack of observations. σ represents the Stefan Boltzmann constant and T_c (K) the inside-canopy temperature. Assuming a linear dependency on canopy fraction, T_c is derived from top-of-canopy temperature T_a (K) as proposed by Obled (1971):

$$T_c = T_a - F_c(T_a - (R_c(T_a - T_{mean}) + T_{mean} - \delta T)), \tag{20}$$

where T_{mean} (K) is the mean daily air temperature, R_c (–) is a dimensionless scaling parameter set to 0.8 and $\delta T\,(-2\,K \leq \delta T \leq +2\,K)$ is a temperature offset defined to be (Durot, 1999)

$$\delta T = \frac{T_{mean} - 273.16}{3}. \tag{21}$$

Durot (1999) has further shown that relative humidity inside the canopy, RH_c (%), is often higher compared to the open due to sublimation and evaporation of melted snow. We therefore propose to modify top-of-canopy humidity RH (%) with consideration of the canopy fraction in the form of (Durot, 1999)

$$RH_c = \max\{RH(1 + 0.1F_c), 100\}. \tag{22}$$

2.5 Simulating canopy effects on the snow cover

The following describes the newly implemented approaches to describe snow interception through the forest canopy as well as melt-induced unloading of intercepted snow from the canopy.

Interception of snow precipitation P (mm), at time t is derived introducing a canopy-intercepted load, I (mm), expressed as (Pomeroy et al., 1998)

$$I = I_{t-1} + 0.7(I_{max} - I_{t-1})(1 - \exp(-P/I_{max})), \tag{23}$$

where $t-1$ represents the previous time step and I_{max} is the maximum interception storage calculated as (Hedstrom and Pomeroy, 1998)

$$I_{max} = 4.4\mathrm{LAI}^*. \tag{24}$$

Sublimation of intercepted snow Q_{cs} (mm) is calculated as described by Liston and Elder (2006b) as

$$Q_{cs} = C_e I \Psi_s dt, \tag{25}$$

where dt (s) is the time increment (here: 3600 s), Ψ_s (s^{-1}) is the sublimation-loss rate coefficient for an ice sphere and C_e(–) represents the canopy exposure coefficient. Ice spheres are assumed to be characterized by a constant radius of 500 µm as proposed by Liston and Elder (2006b).

The canopy exposure coefficient is calculated as

$$C_e = k_c (I/I_{max})^{-0.4}, \tag{26}$$

where k_c (–) is a dimensionless coefficient related to the shape of the intercepted snow deposits (Liston and Elder, 2006b). Sublimation at the canopy scale is hence estimated based on sublimation from individual ice spheres. Analysing observed (Montesi et al., 2004) and modelled sublimation rates for a 2.7 m-tall subalpine fir tree at the USDA Fraser Experimental Forest, Liston and Elder (2006b) have found that the application of $k_c = 0.010$ seems to best reproduce observed sublimation rates at both, higher an lower elevated tree sites. This value is very close to the value of $k_c = 0.011$ derived by Pomeroy et al. (1998) for Canadian Boreal Forest and is used as k_c value for the calculations with ECIMO.spread (v2) here. This parameter can be easily adapted by changing the respective setting in the parameter section of the model.

The sublimation-loss rate coefficient Ψ_s is calculated from the particle mass m (kg) in the form of

$$\Psi_s = (dm/dt)/m, \tag{27}$$

where the particle mass is given by

$$m = \frac{3}{4}\pi \rho_i r^3, \tag{28}$$

GMDD
8, 8155–8191, 2015

with ρ_i ($\mathrm{kg\,m^{-3}}$) being ice density and r (m) representing the radius of a spherical ice particle (assumed to be 500 µm as proposed by Liston and Elder, 2006b).

Mass loss from an ice particle is described as a function of intercepted solar radiation, humidity gradients between the ice surface and the surrounding atmosphere, the size of the considered ice particle and a ventilation term, following Thorpe and Mason (1966) and Schmidt (1972):

$$\frac{\mathrm{d}m}{\mathrm{d}t} = \frac{2\pi\left(\frac{\mathrm{RH}}{100}\right) - S_\mathrm{p}\Omega}{h_\mathrm{s}\Omega + \frac{1}{D\rho_\mathrm{v}Sh}}, \tag{29}$$

where h_s is the latent heat of sublimation ($2.8355 \times 10^6\,\mathrm{J\,kg^{-1}}$).

The diffusivity of water vapour in the atmosphere, D ($\mathrm{m^2\,s^{-1}}$) is derived following Thorpe and Mason (1966) as:

$$D = 2.06 \times 10^{-5}(T_\mathrm{a}/273)^{1.75}. \tag{30}$$

The molecular weight of water M ($18.01\,\mathrm{kg\,kmole^{-1}}$), the universal gas constant R ($8313\,\mathrm{J\,kmole^{-1}\,K^{-1}}$), air temperature T_a (K) and the thermal conductivity of the atmosphere λ_t ($0.024\,\mathrm{J\,m^{-1}\,s^{-1}\,K^{-1}}$) are used to calculate Ω as proposed by Liston and Elder (2006b):

$$\Omega = \frac{1}{\lambda_\mathrm{t} T_\mathrm{a} Nu}\left(\frac{h_\mathrm{s}M}{\mathrm{R}T_\mathrm{a}} - 1\right). \tag{31}$$

The Nusselt number Nu and Sherwood number Sh are both calculated as:

$$Nu = Sh = 1.79 + 0.606Re^{0.5}, \tag{32}$$

where Re ($0.7 < Re < 10$) is the Reynolds number expressed by:

$$Re = \frac{2ru_\mathrm{c}}{v} \tag{33}$$

with ν representing the kinematic viscosity of air ($1.3 \times 10^{-5}\,\mathrm{m^2\,s^{-1}}$) and u_c the ventilation velocity inside the canopy, which is set equal to inside-canopy wind speed as proposed by Liston and Elder (2006b).

Following Fleagle and Businger (1981) the saturation density of water vapor ρ_v ($\mathrm{kg\,m^{-3}}$) is derived as

$$\rho_v = 0.622 \frac{e_s}{R_d T_a} \tag{34}$$

where R_d is the gas constant for dry air ($287\,\mathrm{J\,K^{-1}\,kg^{-1}}$) and e_s (Pa) is the saturation vapor pressure over ice, estimated following Buck (1981) as:

$$e_s = 611.15 \exp\left(\frac{22.452(T_a - 273.16)}{T_a - 0.61}\right). \tag{35}$$

The shortwave radiation absorbed by a snow particle with radius r is defined to be

$$S_p = \pi r^2 (1 - \alpha_p) S_i, \tag{36}$$

where α_p is the snow albedo, and S_i ($\mathrm{W\,m^2}$) is the solar radiation at the earth surface, which in case of ESCIMO.spread (v2) is among the required meteorological input parameters.

To account for a melt-induced unloading of intercepted snow from the canopy, a melt-unloading rate L_m ($\mathrm{kg\,m^{-2}}$) is introduced by Liston and Elder (2006b):

$$L_m = 5.8 \times 10^{-5} (T_a - 273.16) \mathrm{d}t. \tag{37}$$

We assume an unloading rate of $5\,\mathrm{kg\,m^{-2}\,day^{-1}\,K^{-1}}$ whenever temperatures are above freezing, with unloading snow adding to snow accumulation at the land surface. The simulated filling and depletion of the interception storage through snow fall, sublimation and melt induced unload is illustrated in Fig. 4 exemplarily for a period in February 2013.

3 Data and test site description

Snow cover simulations in this study are carried out for the forest site Vordersteinwald in the Black Forest mountain range (south-west Germany) (see Fig. 1). This site is eminently suitable for testing of the newly developed version of ESCIMO.spread as it (i) usually experiences alternation of accumulation and melting periods over the winter season, making the simulation of snow conditions particularly demanding and (ii) has been subject to intense snow surveys over the years 2010–present, including simultaneous observation of meteorological and snow conditions in and outside the forest canopy (Pohl et al., 2014).

The forest stand at the study site is mostly conifer with spruce, fir and pine, representing the most common conifer tree species. To quantify the vegetation effect on snow conditions, the applied snow monitoring systems (SnoMoS) were installed pairwise with one SnoMoS located in the open and another set up in close distance inside the forest canopy (see Fig. 5). The data recorded by these low-cost monitoring sensors include hourly values of snow depth, surface temperature, air temperature and humidity, global radiation, wind speed, and barometric pressure.

The continuous monitoring of snow depth with the SnoMoS was accompanied by bi-weekly snow density surveys that allow translation of snow depth into snow water equivalent. A comprehensive description of the technical specifications and the instrumental setup of the SnoMoS is provided by Pohl et al. (2014). Precipitation recordings for the study site originate from nearby weather station Freudenstadt (DWD, 2015), operated by the German Weather Service (DWD). Precipitation observations have been corrected for differences in terrain elevation between the sites of measurement and model application by applying monthly elevation adjustment factors as proposed by Liston and Elder (2006a). The latter have been taken from Marke (2008) who has investigated altitudinal differences in precipitation for the Upper Danube Watershed. No interpolation using other station data has been carried out due to the closeness of the study site (3 km distance) to station Freudenstadt. Hemispherical images were taken at the forest location and were utilized to derive the effective LAI of the forest stand ($LAI^* = 2.6\,m^2\,m^{-2}$). Moreover, a logarithmic function considering snow ageing and new snowfall was used to compute daily snow densities between the surveys. All data used as model input and for model validation are freely provided along with the model.

4 Results

ESCIMO.spread (v2) has been applied to modify outside-canopy meteorological conditions for canopy effects at site Vordersteinwald as well as for a subsequent simulation of the SWE evolution for the winter season 2012/2013. Figure 6 shows outside-canopy global radiation modified for canopy effects with the new ESCIMO.spread (v2) algorithms in comparison to inside-canopy observations. As global radiation under mid-latitude prealpine conditions usually provides the largest share of energy for snow melt, an accurate representation of inside-forest global radiation is essential for a realistic reproduction of snow ablation with any energy balance model. The general dimension and temporal variation in global radiation inside the forest canopy seem well reproduced with a certain tendency of the model to underestimate global radiation in the forest. This satisfactory model performance is also confirmed by the high values of the coefficient of determination (R^2), the Nash Sutcliffe model efficiency (NSME) and the index of agreement (IA) as provided in Table 1 for all meteorological input variables modified for canopy effects (see Krause et al., 2005 for a detailed explanation of the efficiency criteria applied).

Air temperature is displayed in Fig. 7. The simulated and observed courses of temperature match fairly well until late January, whereas the simulations overestimate daily temperature peaks in spring. The efficiency criteria of R^2, NSME and IA with values of 0.79, 0.82 and 0.94, respectively, further underline the good performance of ESCIMO.spread (v2) with respect to the modification of outside-canopy temperature conditions. Compared to global radiation and temperature, the model performance for relative humidity and wind speed with R^2 and IA values in the order of 0.6 and 0.7–0.8 for both criteria, respectively, is distinctly weaker. In case of both variables the NSME with values below 0 indicates that the mean value of the observations would be a better predictor than the model (Krause et al., 2005). The course of relative humidity and wind speed conditions illustrated in Figs. 8 and 9 explains the diametrical picture of model performance described by means of R^2 and IA compared to NSME. While the temporal variation in relative humidity and wind speed is well reflected in the simulations (resulting in good correlation and acceptable values of R^2 and IA), the exact values in the observed time series are seldomly reproduced by the model results, a condition that is considered in the calculation of NSME (Krause et al., 2005). The high temporal and spatial variability in wind speed naturally makes any spatial interpolation or modification for canopy effects particularly challenging. In case of both variables, the simulations tend to exceed observed values of humidity and wind speed in the forest canopy.

The simulated snow cover is displayed in Fig. 10 for the open and in Fig. 11 for inside the canopy in comparison to observations at the respective sites. The dark-grey and light-grey line represent the simulations achieved using observed meteorological conditions inside the canopy (as provided by the SnoMoS inside the forest) and meteorological conditions derived through modification of outside meteorological conditions (as provided by the SnoMoS in the open) as input for the model, respectively. Due to a lack of precipitation recordings inside the forest, the precipitation data used as input for the simulations inside the canopy in both cases represent recordings from station Freudenstadt modified for canopy effects. Hence, precipitation inside the canopy as used as input for the snow simulations has to be considered a model result rather than an observation. Snow cover evolution is nevertheless reasonably reproduced by the model in- and outside the forest canopy with a distinct overestimation of snow water equivalent between 15 and 26 December. A closer look at the conditions during this period reveals significant snowfall at temperatures close to 0 °C and air humidity close to saturation. Hence, an explanation for the observed overestimation of snow water equivalent in this period might be a false interpretation of rainfall as snowfall. While the model acceptably reproduces snow accumulation between 10 and 30 January in the open, a noticeable overestimation of snow water equivalent can be observed in the results using the modified outside-canopy meteorological conditions. While a period of snow accumulation can be observed in the observations and simulations for the open in March, inside the canopy this increase in snow water equivalent is merely predicted by the model and not confirmed by the observations. A comparison of the snow simulations based on observed and simulated meteorological conditions inside the canopy reveals that only little differences exist between both model runs, with the model performance using observed meteorological conditions as model input being slightly better. Taking a closer look at the efficiency criteria in Table 2, the model results for both locations seem to well reflect the observed conditions with model performance inside the canopy beeing even slightly better than in the open.

5 Conclusions

A new version of the spreadsheet-based point energy balance snow model ESCIMO.spread has been presented (ESCIMO.spread (v2)) that allows an improved precipitation phase detection, consideration of cold and liquid water content in the snow cover, estimation of inside canopy meteorological conditions from meteorological observations in the open and the simulation of snow accumulation and ablation inside a forest canopy. It thereby does not require meteorological observations in the canopy but instead derives inside-canopy meteorological conditions from available observations in the open requiring only LAI and canopy height as plant-specific input parameters. The derived meteorological conditions inside the canopy are not only applicable as input for snow cover simulations but can be expected to be of interest for a variety of scientific disciplines, e.g. forest ecology or pedology. To provide the data required for model application and evaluation, a pair of SnoMoS has been utilized as an innovative technology that allows the collection of important meteorological variables at low financial costs. Comparison of simulated inside-canopy meteorological conditions to observations at a site in the Black Forest region (Germany) reveals good overall model performance, particularly with respect to global radiation and temperature representing the most important meteorological variables for the estimation of snow melt. A similar picture unfolds when comparing the simulated snow cover evolution in- and outside the canopy to snow observations provided by the SnoMoS. Here, snow cover evolution is well reproduced for both, out- and inside the forest canopy, with slightly higher model performance for inside-canopy conditions, even though the empirical model parameters have not yet been adjusted to (pre)alpine forest species. Making use of the full potential of simultaneous observation of snow and meteorological conditions as provided by the SnoMoS, an effort is currently undertaken to develop parameters for the applied canopy model that are tailored to the specific conditions in (pre)alpine forests. Moreover, despite its physically-based character and advanced model features, ESCIMO.spread (v2) still oversimplifies some important processes of the snow-vegetation interaction. In the current version the model only considers unloading of intercepted snow as a result of melting. While the fact that wind also induces unloading of intercepted snow is well known, the combined dependence on plant characteristics (e.g. plant structure and plant element flexibility) and meteorological conditions (e.g. snow temperature, wind speed and direction) makes this a complex process hard to consider in numerical models (Liston and Elder, 2006b). The modification of shortwave and longwave radiation assumes a plant specific extinction coefficient and a constant canopy fraction, respectively. While these assumptions can be expected to reasonably reproduce the general observed trends in local radiation, they are not capable to accurately capture the actual radiation conditions whenever canopy densities strongly vary or sun is shining through open areas in the trees as a result of changing solar zenith angles.

GMDD
8, 8155–8191, 2015

Code availability

ESCIMO.spread (v2) can be downloaded free of charge at www.alpinehydroclimatology.net together with one year of sample data including the meteorological and snow observations used in this study. The model has been tested on OpenOffice 4.1.1. as well as on different versions of Microsoft Excel for Windows and Mac.

Acknowledgements. The authors thank the Austrian Climate and Energy Fund for the financial support of the presented research (ACRP6 – STELLA – KR13AC6K11109) within the Austrian Climate Research Programme. Moreover, we thank the German Weather Service (DWD) for the provision of the precipitation recordings at Station Freudenstadt.

References

Blöschl, G. and Kirnbauer, R.: Point snowmelt models with different degrees of complexity – internal processes, J. Hydrol., 129, 127–147, 1991. 8162

Braun, L. N.: Simulation of Snowmelt-Runoff in Lowland and Lower Alpine Regions of Switzerland, PhD thesis, ETH Zurich, Zürich, 1984. 8162

Breuer, L., Eckhardt, K., and Frede, H.-G.: Plant parameter values for models in temperate climates, Ecol. Model., 169, 237–293, 2003. 8164

Brock, B. W. and Arnold, N. S.: A spreadsheet-based (Microsoft Excel) point surface energy balance model for glacier and snow melt studies, Earth Surf. Proc. Land., 25, 649–658, 2000. 8158

Buck, A. L.: New equations for computing vapor pressure and enhancement factor, J. Appl. Meteorol., 20, 1527–1532, 1981. 8169

Campbell, G. S. and Norman, J. M.: An Introduction to Environmental Biophysics, Springer, New York, 1998. 8161

Chen, J. M., Rich, P. M., Gower, S. T., Norman, J. M., and Plummer, S.: Leaf area index of boreal forests: theory, techniques, and measurements, J. Geophys. Res., 102, 29429–29443, doi:10.1029/97JD01107, 1997. 8164

GMDD
8, 8155–8191, 2015

A spreadsheet-based snow model for inside-canopy conditions

T. Marke et al.

Cionco, R. M.: Analysis of canopy index values for various canopy densities, Bound.-Lay. Meteorol., 15, 81–93, 1978. 8164

Dickerson-Lange, S. E., Lutz, J. A., Martin, K. A., Raleigh, M. S., Gersonde, R., and Lundquist, J. D.: Evaluating observational methods to quantify snow duration under diverse forest canopies, Water Resour. Res., 51, 1203–1224, doi:10.1002/2014WR015744, 2015. 8157

Durot, K.: Modélisation hydrologique distribuée du bassin versant nivo–pluvial de Sarennes, Validation des données d'entrée et dévelopement d'un module de fonte nivale sous forêt, PhD thesis, LTHE, Grenoble, 1999. 8166

DWD: Precipiatation Dataset from Station Freudenstadt, German Weather Service (DWD), Offenbach am Main, ftp://ftp-cdc.dwd.de/pub/CDC/observations_germany/climate/hourly/, last access: 18 September 2015. 8170

Essery, R., Pomeroy, J., Parviainen, J., and Storck, P.: Sublimation of snow from coniferous forests in a climate model, J. Climate, 16, 1855–1864, 2003. 8164

Fleagle, R. G. and Businger, J. A.: An Introduction to Atmospheric Physics, 2 edn., Cambridge University Press, Cambridge, 1981. 8169

Hardy, J. P., Melloh, R., Robinson, P., and Jordan, R.: Incorporating effects of forest litter in a snow process model, Hydrol. Process., 14, 3227–3237, 2001. 8157

Hedstrom, N. R. and Pomeroy, J. W.: Measurements and modelling of snow interception in the boreal forest, Hydrol. Process., 12, 1611–1625, 1998. 8166

Hellström, R.: Forest cover algorithms for estimating meteorological forcing in a numerical snow model, Hydrol. Process., 14, 3239–3256, 2001. 8165

Kraus, H.: Die Atmosphäre der Erde – eine Einführung in die Meteorologie, Springer, Heidelberg, 2004. 8161

Krause, P., Boyle, D. P., and Bäse, F.: Comparison of different efficiency criteria for hydrological model assessment, Adv. Geosci., 5, 89–97, doi:10.5194/adgeo-5-89-2005, 2005. 8171, 8172

Link, T. and Marks, D.: Distributed simulation of snowcover mass- and energy-balance in the boreal forest, Hydrol. Process., 13, 2439–2452, 1999a. 8157

Link, T. E. and Marks, D.: Point simulation of seasonal snow cover dynamics beneath boreal forest canopies, J. Geophys. Res., 104, 27841–27857, doi:10.1029/1998JD200121, 1999b. 8157

Liston, G. E. and Elder, K.: A meteorological distribution system for high-resolution terrestrial modeling (MicroMet), J. Hydrometeorol., 7, 217–234, 2006a. 8165, 8166, 8170

Liston, G. E. and Elder, K.: A distributed snow-evolution modeling system (SnowModel), J. Hydrometeorol., 7, 1259–1276, 2006b. 8157, 8164, 8165, 8167, 8168, 8169, 8174

Marke, T.: Development and Application of a Model Interface to Couple Land Surface Models with Regional Climate Models for Climate Change Risk Assessment in the Upper Danube Watershed, PhD thesis, Ludwig-Maximilians-University, Munich, 2008. 8170

Marsh, P.: Snowcover formation and melt: recent advances and future prospects, Hydrol. Process., 13, 2117–2134, 1999. 8156

Melloh, R. A., Hardy, J. P., Davis, R. E., and Robinson, P. B.: Spectral albedo/reflectance of littered forest snow during the melt season, Hydrol. Process., 15, 3409–3422, 2002. 8157

Montesi, J., Elder, K., Schmidt, R. A., and Davis, R. E.: Sublimation of intercepted snow within a subalpine forest canopy at two elevations, J. Hydrometeorol., 763–773, doi:10.1175/1525-7541(2004)005<0763:SOISWA>2.0.CO;2, 2004. 8167

Obled, C.: Modèles mathématiques de la fusion nivale, PhD thesis, Université Scientifique et Médicale de Grenoble, Grenoble, 1971. 8166

Pohl, S., Garvelmann, J., Wawerla, J., and Weiler, M.: Potential of a low-cost sensor network to understand the spatial and temporal dynamics of a mountain snow cover, Water Resour. Res., 50, 2533–2550, 2014. 8157, 8159, 8170

Pomeroy, J. and Gray, D. M.: Snowcover: Accumulation, Relocation, and Management, Tech. Rep. 7, National Hydrology Research Institute, National Hydrology Research Institute Science Report No. 7, Saskatoon, Canada, 1995. 8157

Pomeroy, J. W., Parviainen, J., Hedstrom, N., and Gray, D. M.: Coupled modelling of forest snow interception and sublimation, Hydrol. Process., 12, 2317–2337, 1998. 8156, 8166, 8167

Pomeroy, J. W., Gray, D. M., Hedstrom, N. R., and Janowicz, J. R.: Prediction of seasonal snow accumulation in cold climate forests, Hydrol. Process., 16, 3543–3558, 2002. 8157

Schmidt, R. A.: Sublimation of Wind-Transported Snow: a Model, Tech. rep., USDA Forest Service research paper, Rocky Mountain Forest and Range Experiment Station, Fort Collins, CO, 1972. 8168

Steinacker, R.: Diagnose und Prognose der Schneefallgrenze, Wetter und Leben, 35, 81–90, 1983. 8160

Strasser, U.: Modelling of the mountain snow cover in the Berchtesgaden National Park, Forschungsberichte des Nationalpark Berchtesgaden, 55, 1–184, 2008. 8164

Strasser, U. and Marke, T.: *ESCIMO.spread* – a spreadsheet-based point snow surface energy balance model to calculate hourly snow water equivalent and melt rates for historical and

GMDD
8, 8155–8191, 2015
A spreadsheet-based snow model for inside-canopy conditions
T. Marke et al.

Title Page
Abstract | Introduction
Conclusions | References
Tables | Figures
◀| |▶
◀ ▶
Back | Close
Full Screen / Esc
Printer-friendly Version
Interactive Discussion

changing climate conditions, Geosci. Model Dev., 3, 643–652, doi:10.5194/gmd-3-643-2010, 2010. 8157, 8159, 8160

Strasser, U., Bernhardt, M., Weber, M., Liston, G. E., and Mauser, W.: Is snow sublimation important in the alpine water balance?, The Cryosphere, 2, 53–66, doi:10.5194/tc-2-53-2008, 2008. 8157

Strasser, U., Warscher, M., and Liston, G. E.: Modeling snow canopy processes on an idealized mountain, J. Hydrometeorol., 12, 663–677, 2011. 8157, 8164

Thorpe, A. D. and Mason, B. J.: The evaporation of ice spheres and ice crystals, Briti. J. Appl. Phys., 17, 541–548, 1966. 8168

Walter, M. T., Brooks, E. S., McCool, D. K., King, L. G., Molnau, M., and Boll, J.: Process-based snowmelt modeling: does it require more input data than temperature-index modeling?, J. Hydrol., 300, 65–75, 2005. 8158

Table 1. Performance of ESCIMO.spread (v2) in the modification of outside-canopy global radiation, temperature, relative humidity and wind speed for canopy effects.

Variable	NSME	R^2	IA
Global radiation	0.64	0.66	0.89
Air temperature	0.79	0.82	0.94
Relative humidity	−1.10	0.61	0.74
Wind speed	−0.29	0.60	0.78

GMDD
8, 8155–8191, 2015

Table 2. Performance of ESCIMO.spread (v2) in the simulation of snow cover evolution in- and outside the forest canopy. The simulations inside the canopy are based on modified outside-canopy meteorological conditions.

Variable	NSME	R^2	IA
SWE (outside canopy)	0.65	0.77	0.88
SWE (inside canopy)	0.80	0.82	0.95

GMDD
8, 8155–8191, 2015

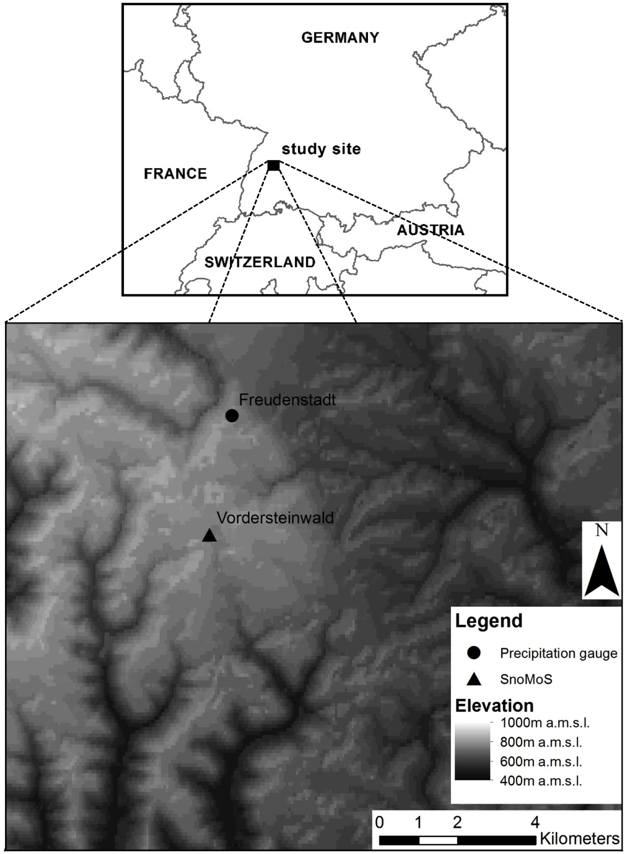

Figure 1. The site Vordersteinwald in the Black Forest mountain range (south-west Germany, 800 m a.s.l).

GMDD
8, 8155–8191, 2015

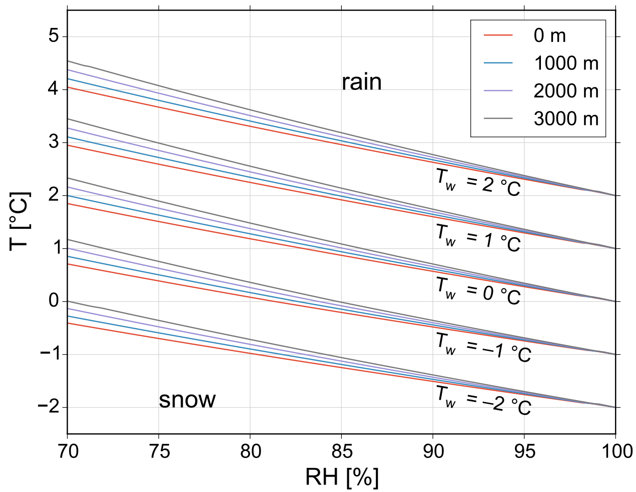

Figure 2. Relation between air temperature, wet-bulb temperature and relative humidity in different altitudes. The latter represent different air pressure levels derived using the hydrostatic equation.

GMDD

8, 8155–8191, 2015

A spreadsheet-based snow model for inside-canopy conditions

T. Marke et al.

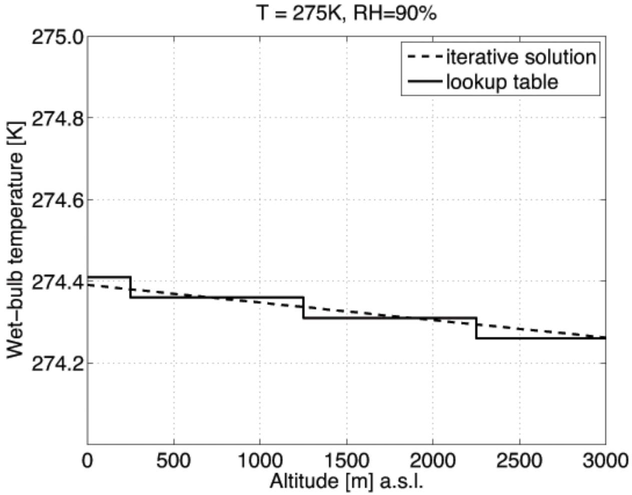

Figure 3. Comparison of iteratively calculated wet bulb temperature to the results of the lookup table approach implemented in ESCIMO.spread (v2).

GMDD
8, 8155–8191, 2015

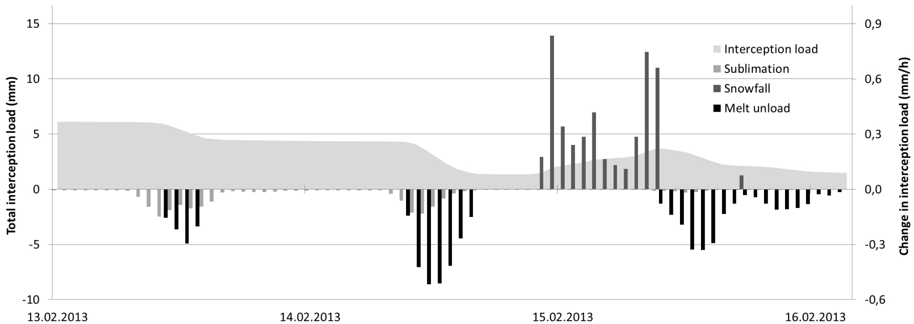

Figure 4. Simulated filling and depletion of the interception storage through snowfall, sublimation and melt induced unload at site Vordersteinwald in the Black Forest mountain range (south-west Germany).

GMDD
8, 8155–8191, 2015

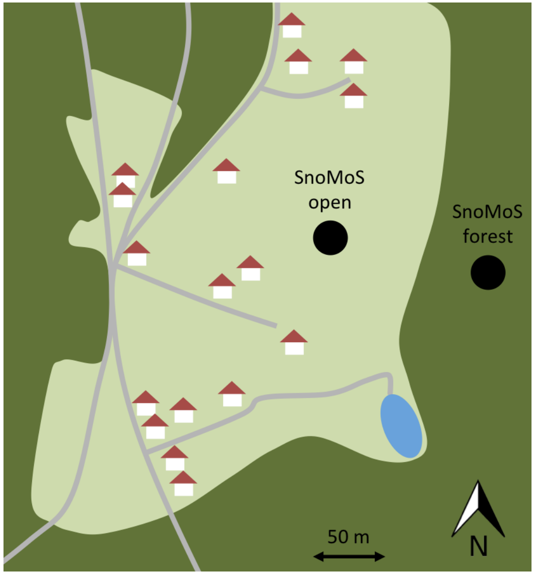

Figure 5. Schematic overview of the SnoMoS setup locations in- and outside the forest canopy at site Vordersteinwald in the Black Forest mountain range (south-west Germany, 800 m a.s.l). The light green areas indicate grassland, the dark green areas forest, the grey lines streets and the light blue area a lake.

GMDD
8, 8155–8191, 2015

A spreadsheet-based snow model for inside-canopy conditions

T. Marke et al.

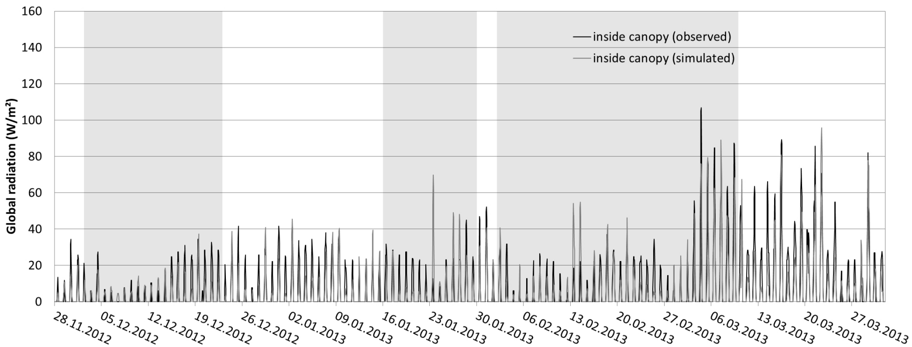

Figure 6. Simulated and observed global radiation for the winter period 2012/13. The grey areas indicate periods with presence of a snow cover.

GMDD
8, 8155–8191, 2015

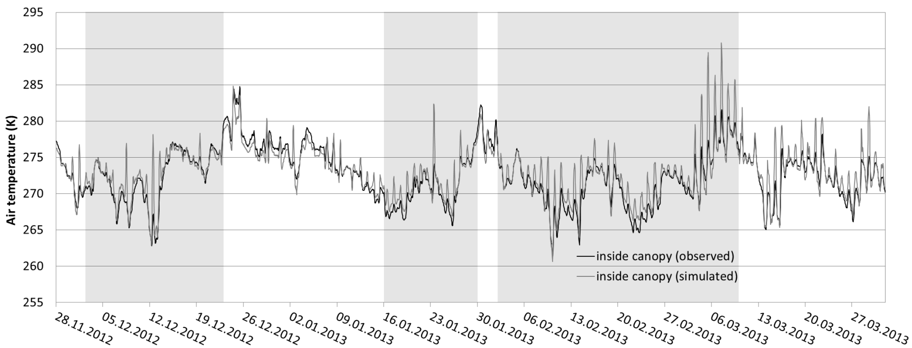

Figure 7. Simulated and observed temperature inside the forest canopy for the winter period 2012/13. The grey areas indicate periods with presence of a snow cover.

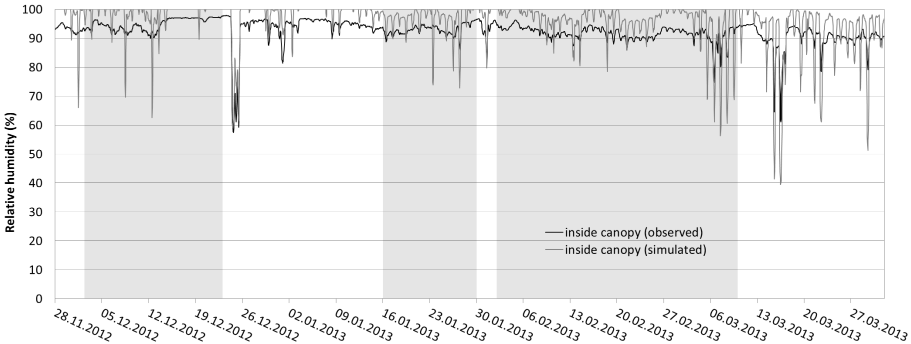

Figure 8. Simulated and observed relative humidity inside the forest canopy for the winter period 2012/13. The grey areas indicate periods with presence of a snow cover.

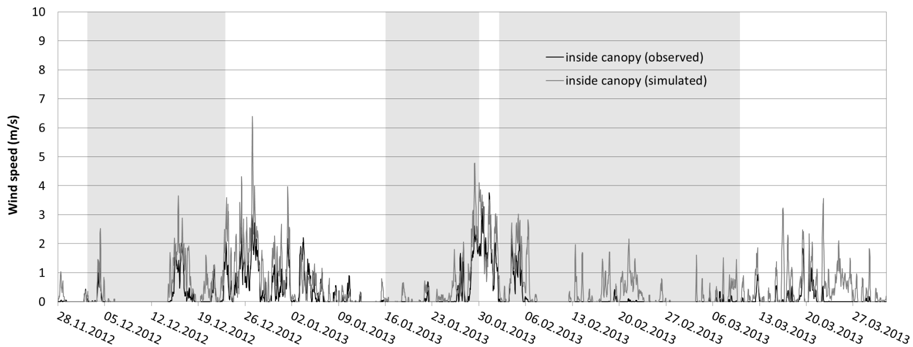

Figure 9. Simulated and observed wind speed inside the forest canopy for the winter period 2012/13. The grey areas indicate periods with presence of a snow cover.

GMDD
8, 8155–8191, 2015

A spreadsheet-based snow model for inside-canopy conditions

T. Marke et al.

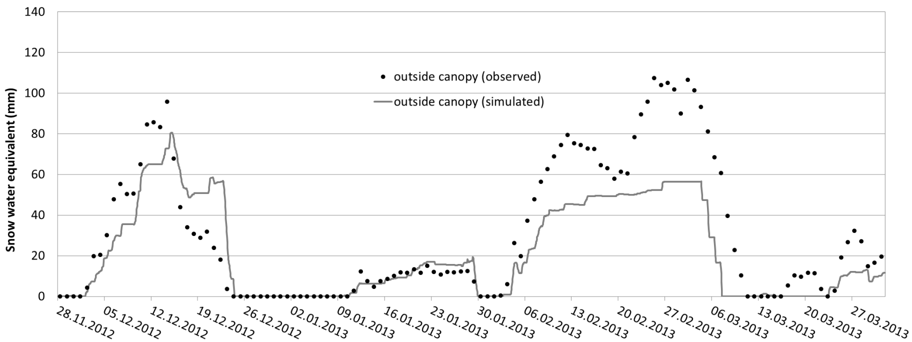

Figure 10. Simulated and observed snow water equivalent outside the forest canopy for the winter period 2012/13.

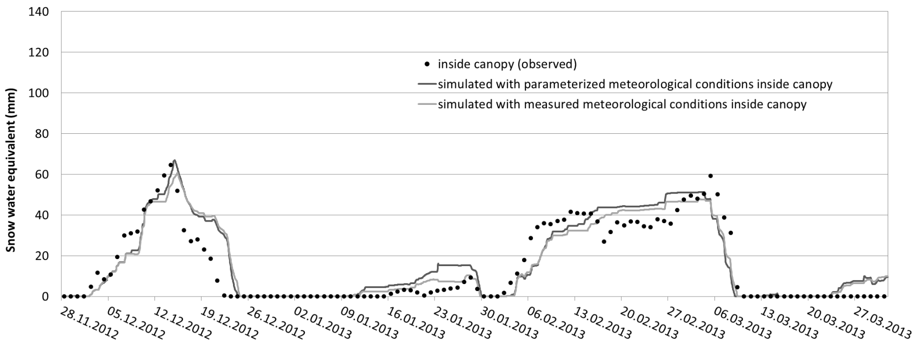

Figure 11. Simulated and observed snow water equivalent inside the forest canopy for the winter period 2012/13. The two curves illustrate the snow simulations achieved with the parameterized (dark grey line) and observed (light grey line) meteorological conditions inside the canopy.

GMDD
8, 8155–8191, 2015